PoS(SMPRI2005)026

Energetics of a simple microscopic heat engine

Mesfin Asfaw and Mulugeta Bekele[*]

Department of Physics, Addis Abeba University, P.O. Box 1176, Addis Abeba, Ethiopia
E-mail: `malefya@yahoo.com`

We model a microscopic heat engine as a particle hopping on a one-dimensional lattice in a periodic sawtooth potential, with or without load, assisted by the thermal kicks it gets from alternately placed hot and cold thermal baths. We find analytic expressions for current and rate of heat flow when the engine operates at steady state. Three regions are identified where the model acts either as a heat engine or as a refrigerator or as neither of the two. At quasistatic limit both efficiency of the engine and coefficient of performance of the refrigerator go to that for Carnot engine and Carnot refrigerator, respectively. We investigate efficiency of the engine at two operating conditions (at maximum power and at optimum value with respect to energy and time) and compare them with those of the endoreversible and Carnot engines.

[*]Speaker.

1. Introduction

Even though both macroscopic as well as microscopic heat engines work on the same thermodynamic principles, wide-ranging studies have been done in improving the performance of macroscopic heat engines [1]. At present, the study of microscopic heat engines has received considerable attention [3, 2]. This is because of the trend in miniaturization and the need to utilize energy resources available at microscopic scales. As such, modelling microscopic heat engines and finding how well they perform is a primary task to be undertaken at present.

To get a first insight as to how such engines perform, it is important to take a toy model that has the basic ingredients. In a recent paper [4] we considered a simple model of a Brownian heat engine and found exact analytic expressions for quantities like current, efficiency and coefficient of performance. This, in turn, enabled us to explore different features of the engine such as efficiency at maximum power, optimized efficiency as well as efficiency at quasistatic limit. The present work addresses the same basic issues of a tiny heat engine. However, here the particle moves on a discrete lattice by hopping as opposed to a continuous Brownian motion in a viscous medium. Even though the model and its corresponding dynamics is completely different from the one previously studied, the results can be compared with those of the previous work at least qualitatively. As such, this work can be taken as an independent check of the results found in the previous work on microscopic heat engine.

The paper is organized as follows: In section II, we will first introduce our model in the absence of external load and set up the dynamics governing it. We will then find analytic expressions for the steady-state current and the rate of heat produced as a function of the model parameters. In section III, we will consider our model in the presence of an external load and find the steady-state current and the rate of heat flows. In section IV, expressions for the efficiency and coefficient of performance (COP) will be determined depending on whether the engine works as a heat engine or as a refrigerator. Regions in the parameter space where the model works as a heat engine, as a refrigerator and as neither of the two will be determined. We will explore how current, efficiency and COP behave as the model parameters vary. We will also compare the efficiency of the engine at two operating conditions (at maximum power and at optimum value with respect to energy and time) with those of endoreversible and Carnot engines. Lastly, we summarize and conclude in section V.

2. Zero external load

The model we take is a modified version of the one considered by Jarzynski and Mazonka [5] in modelling Feynman's ratchet and pawl system. Mimicking the original Feynman's ratchet and pawl system [6], Jarzynski and Mazonka [5] considered a particle in a ratchet potential which is *simultaneously* in contact with hot and cold heat reservoirs. On the other hand, our model considers a particle in a ratchet potential which is *alternately* in contact with hot and cold reservoirs as it moves along its path.

Consider a particle that moves by hopping on a one-dimensional lattice, with lattice spacing d, assisted by the thermal kick it gets from periodically placed hot and cold reservoirs along its path. The particle is also exposed to an external discrete sawtooth potential which has the same period as
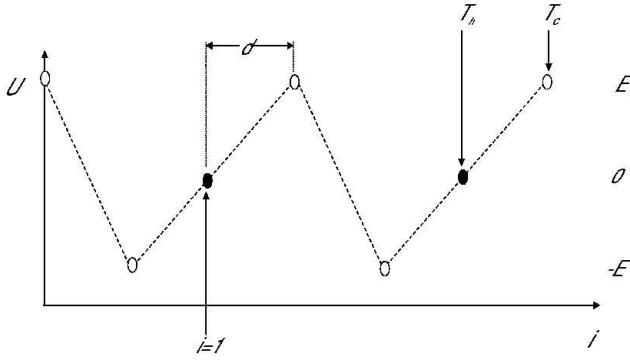
Figure 1: Plot of discrete sawtooth potential without load. Sites with dark circles are coupled to the hot reservoir (T_h) while sites with open circles are coupled to the cold reservoir (T_c). Site 1 is labeled explicitly and d is the lattice spacing.

that of the reservoirs. In one cycle, the particle walks a net displacement of three lattice sites, either to the right or to the left. This corresponds to the particle crossing one sawtooth of a sawtooth potential. The potential energy at site i, U_i, where i is an integer that runs from $-\infty$ to $+\infty$, is given by

$$U_i = E[i(\text{mod})3 - 1].\tag{2.1}$$

Here E is positive constant having a unit of energy.

The temperature profile at site i, T_i, is given by

$$T_i = \begin{cases} T_h, & \text{if } [i(\text{mod})3 \text{ - } 1] = 0, \\ T_c, & \text{otherwise,} \end{cases}\tag{2.2}$$

where T_h and T_c are the temperatures of the hot and cold reservoirs, respectively. Figure 1 shows the values of sawtooth potential and of the temperature at the given lattice sites.

The jump of the particle from one lattice site to next lattice site is assumed to be random in nature. The jump probability is determined by the amount of energy it crosses and the temperature of the heat reservoir to which it is coupled. Accordingly, the jump probability per unit time of the particle making a jump from site i to site $i+1$ is given by $\Gamma e^{\frac{-\Delta E}{T_i}}$, where $\Delta E = U_{i+1} - U_i$ and Γ is the probability that the particle will attempt a jump per unit time. We take Boltzmann's constant, k_B, to be unity. When the particle attempts to jump, first it decides which way to jump (either to the left or right) with equal probability and then jumps according to the Metropolis algorithm [7]: if the value of $\Delta E \leq 0$, then the jump definitely takes place; if $\Delta E > 0$ then the jump takes place with probability $exp(\frac{-\Delta E}{T_i})$.

The dynamics of the model can be studied by mapping the model to a spin-1 particle system which exhibits identical behavior [5]. Denoting the spin states, s, by $(0, \pm 1)$, the energy function of the spin-1 particle is defined by

$$E(s) = Es.\tag{2.3}$$

The change of state of spin s corresponds to the jump of the particle. If s changes from -1 to 0 or from 0 to 1 or from 1 to -1, then this is the same as the particle jumping to the right. The reverse process corresponds to jump to the left.

The dynamics of the particle is then described by stochastic jumps among the three states. The process is Markovian and we can describe the evolution of the states with rate equations. To the three spin states $s = -1, 0$ and 1 we denote three corresponding states $n = 1, 2$ and 3. Let the probability for the particle to be found in state n at time t be given by $p_n(t)$. The rate equations governing the evolution of the three states are

$$\frac{dp_n}{dt} = \sum_{n' \neq n} (P_{nn'} p_{n'} - P_{n'n} p_n), n, n' = 1, 2, 3. \tag{2.4}$$

$P_{n'n}$ is the transition probability rate at which the particle, originally in state n, makes transition to state n'. Here $P_{n'n}$ is given by the Metropolis rule. For example,

$$P_{21} = \frac{\Gamma}{2} e^{\frac{-E}{T_c}}, \; P_{12} = \frac{\Gamma}{2}, \; P_{32} = \frac{\Gamma}{2} e^{\frac{-E}{T_h}}, \; P_{23} = \frac{\Gamma}{2}. \tag{2.5}$$

Note that state $n = 2$ is coupled to the hot reservoir. In the above expressions, the factor $\frac{1}{2}$ is due to the decision for the particle to jump either to the left or to the right. The rate equation for the model can then be expressed as a matrix equation

$$\frac{d\vec{p}}{dt} = \Gamma \mathbf{R} \vec{p} \tag{2.6}$$

where $\vec{p} = (p_1, p_2, p_3)^T$. Here, $\mathbf{R}$ is a 3 by 3 matrix which is given by

$$\mathbf{R} = \begin{pmatrix} \frac{-\mu - \mu^2}{2} & \frac{1}{2} & \frac{1}{2} \\ \frac{\mu}{2} & \frac{-1-\nu}{2} & \frac{1}{2} \\ \frac{\mu^2}{2} & \frac{\nu}{2} & -1 \end{pmatrix}, \tag{2.7}$$

where $\mu = e^{\frac{-E}{T_c}}$ and $\nu = e^{\frac{-E}{T_h}}$. Note that the sum of each column of the matrix $\mathbf{R}$ is zero, $\sum_m \mathbf{R}_{mn} = 0$. This shows that the total probability is conserved: $\frac{d}{dt} \sum_n p_n = \frac{d}{dt} (\mathbf{1}^T . \vec{p}) = \mathbf{1}^T . (\Gamma \mathbf{R} \vec{p}) = 0$.

The steady state probability distribution $\bar{\vec{p}}$ of Eq. (6) is obtained by solving $\mathbf{R} \bar{\vec{p}} = 0$. We find the normalized $\bar{\vec{p}}$ to have components given by

$$\bar{p}_1 = \frac{1}{1 + \mu + \mu^2}, \tag{2.8}$$

$$\bar{p}_2 = \frac{2\mu + \mu^2}{(2 + \nu)(1 + \mu + \mu^2)}, \tag{2.9}$$

$$\bar{p}_3 = \frac{(2 + \nu)(\mu^2 + \mu) - (2\mu + \mu^2)}{(2 + \nu)(1 + \mu + \mu^2)}. \tag{2.10}$$

The presence of the hot and cold regions along the lattice leads to unidirectional steady state current, J. This steady state current, J, can be found as the difference between the current towards the right, J^+, and the current towards the left, J^-, between any two states: $J = J^+ - J^-$. Selecting processes taking place between states 2 and 3, the current towards the right, J^+, is given by

$$J^+ = \Gamma(R_{32} \bar{p}_2), \tag{2.11}$$

while the current towards the left, J^-, is given by

$$J^- = \Gamma(R_{23}\bar{p}_3). \tag{2.12}$$

After some algebra the explicit expression for the current J takes a simple form

$$J = \frac{\Gamma\mu(\nu - \mu)}{2(2+\nu)(1+\mu+\mu^2)}. \tag{2.13}$$

In each cycle, the particle walks a net displacement of three lattice sites, 3d. Therefore the drift velocity, v, of the particle is

$$v = 3dJ. \tag{2.14}$$

Notice that the net current is to the right as long as $T_h > T_c$ and zero when $T_h = T_c$.

Let us next find the amount of heat transfer per cycle between the hot and cold reservoirs as the particle climbs up or down the potential. We assume the case where there is no energy transfer via kinetic energy due to particle recrossing of the boundary between the hot and cold reservoirs [8, 9]. When the particle jumps from state 2 to state 3, it takes heat from the hot reservoir whose amount is sufficient to climb up the potential energy difference between the states and equal to E. When the particle jumps from state 3 to state 2, it gives heat to the hot reservoir by losing its potential energy and is equal to E. Thus, the net heat per unit time taken from the hot reservoir due to climbing up or down the potential, $\dot{Q}_h$, is given by

$$\dot{Q}_h = E\Gamma(R_{32}\bar{p}_2 - R_{23}\bar{p}_3). \tag{2.15}$$

Using Eqs. (11), (12) and (13) in Eq. (15), we get

$$\dot{Q}_h = EJ. \tag{2.16}$$

When the particle jumps from state 3 to state 1 and from state 2 to state 1, it gives heat to the cold reservoir. When it jumps from state 1 to state 3 and from state 1 to state 2, it takes heat from the cold reservoir. The net heat per unit time given to the cold reservoir due to climbing up or down the potential is given by

$$\dot{Q}_c = E\Gamma(2R_{13}\bar{p}_3 - 2R_{31}\bar{p}_1 + R_{12}\bar{p}_2 - R_{21}\bar{p}_1). \tag{2.17}$$

After substituting the values of $\bar{p}_i$'s and R_{ij}'s, we obtain

$$\dot{Q}_c = EJ. \tag{2.18}$$

The above results show that $\dot{Q}_c = \dot{Q}_h$. This clearly shows that the amount of heat taken from the hot reservoir directly goes to the cold reservoir without doing any work. This is in contrast to the result we found in our previous paper [4] where work is done against viscous medium even in the absence of external load. In the present lattice model, the reservoirs are placed on the lattices that are of measure zero. Hence, there is no dissipation.

Let us now compute the rate of entropy production. The rate of entropy production related with the flow of heat from the hot reservoir is given by $\dot{S}_h = \frac{-\dot{Q}_h}{T_h}$ while the rate of entropy production
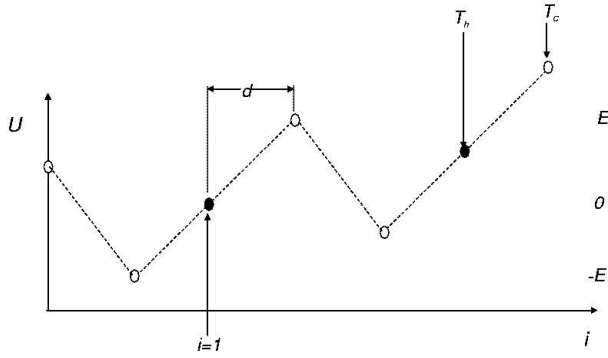
Figure 2: Plot of discrete sawtooth potential with load along with the discrete temperature profile on the lattice

related with the flow of heat to the cold reservoir is: $\dot{S}_c = \frac{\dot{Q}_c}{T_c}$. The net rate of entropy production given by $\dot{S} = \dot{S}_h + \dot{S}_c$ takes of the form,

$$\dot{S} = J\ln\left(\frac{v}{\mu}\right) \geq 0. \tag{2.19}$$

Notice that $\dot{S}$ is non-negative which implies that the system is consistent with the second law of thermodynamics.

3. Non-zero external load

Let us consider the model in the presence of constant external load, f, added to the sawtooth potential as shown in Fig. 2. Accordingly, the potential energy will now be changed from U_i to $U_i + ifd$. The method of solving for steady state behavior is the same as that for the load-free case. We consider our model when the load, f, is greater than zero and for Metropolis algorithm to hold, we need to limit the range of f to $0 < f < \frac{2E}{d}$. For this range of the load, we find the matrix **R**,

$$\mathbf{R} = \begin{pmatrix} -\frac{\mu a}{2} - \frac{\mu^2}{2a} & \frac{1}{2} & \frac{1}{2} \\ \frac{\mu a}{2} & \frac{-1-vb}{2} & \frac{1}{2} \\ \frac{\mu^2}{2a} & \frac{vb}{2} & -1 \end{pmatrix}, \tag{3.1}$$

where $a = e^{\frac{-f.d}{T_c}}$ and $b = e^{\frac{-f.d}{T_h}}$. Note that the sum of each column of the matrix **R** is zero, which shows that the total probability is conserved. The steady state probability $\bar{p}$ satisfies the matrix equation, $\mathbf{R}\bar{p} = 0$. We solve for $\bar{p}$ and after normalization the final results are of the form:

$$\bar{p}_1 = \frac{1}{1 + \mu a + \frac{\mu^2}{a}}, \tag{3.2}$$

$$\bar{p}_2 = \frac{2\mu a + \frac{\mu^2}{a}}{(2 + vb)(1 + \mu a + \frac{\mu^2}{a})}, \tag{3.3}$$

$$\bar{p}_3 = \frac{(2 + vb)(\frac{\mu^2}{a} + \mu a) - (2a\mu + \frac{\mu^2}{a})}{(2 + vb)(1 + \mu a + \frac{\mu^2}{a})}. \tag{3.4}$$

Using similar approach as in section II, the expressions for the steady state current, J, and the drift velocity, v, are respectively found to be given by

$$J = \frac{\Gamma\mu(bav - \frac{\mu}{a})}{2(2+vb)(1+a\mu+\frac{\mu^2}{a})},$$ (3.5)

and

$$v = 3dJ.$$ (3.6)

When the Brownian particle walks along the potential with additional load, it takes heat from the hot reservoir and gives some part of it to the cold reservoir and uses the rest for climbing up the load. The difference between the rate of heat energy that the Brownian particle takes from the hot reservoir, $\dot{Q}_h$, and the rate of heat energy that it gives to the cold reservoir, $\dot{Q}_c$, is the rate of useful work, $\dot{W}$, that the particle uses to lift the load; i.e,

$$\dot{W} = \dot{Q}_h - \dot{Q}_c = fv.$$ (3.7)

The expressions for $\dot{Q}_h$ and $\dot{Q}_c$ can be obtained by a similar approach as in section II and we find them to be given by

$$\dot{Q}_h = (E + fd)J.$$ (3.8)

and

$$\dot{Q}_c = (E - 2fd)J.$$ (3.9)

The difference, $\dot{Q}_h - \dot{Q}_c$, will then be

$$\dot{Q}_h - \dot{Q}_c = 3fdJ = fv,$$ (3.10)

which is exactly equal to $\dot{W}$ as given in Eq. (26).

4. The model as a heat engine, as a refrigerator and as neither of the two

To specify the model, one requires to specify the six quantities: Γ, d, E, T_c, T_h and f. Taking Γ, d and T_c fixed we still have three parameters E, T_h and f that can be varied independently. We convert these into three dimensionless parameters ε, τ and λ where $\varepsilon = \frac{E}{T_c}$, $\tau = \frac{T_h}{T_c} - 1$ and $\lambda = \frac{fd}{T_c}$. In addition, we introduce a dimensionless current $j = \frac{J}{\Gamma}$. We take $T_h > T_c$ for the rest of our work.

The current j is now a function of ε, τ and λ. Figure 3 shows a plot of j versus λ for fixed values of ε and τ. The figure shows that the current is positive as long as the load is less than a certain value of λ. This corresponds to the region where the model works as a heat engine. Using Eqs. (27), (28) and (29) the efficiency of the heat engine, η, takes the expression

$$\eta = \frac{\dot{Q}_h - \dot{Q}_c}{\dot{Q}_h} = \frac{3\lambda}{(\varepsilon + \lambda)}.$$ (4.1)

On the other hand, when the load is large enough the current becomes negative and that implies that the model works as a refrigerator. The COP, P_{ref}, of the refrigerator then takes the expression

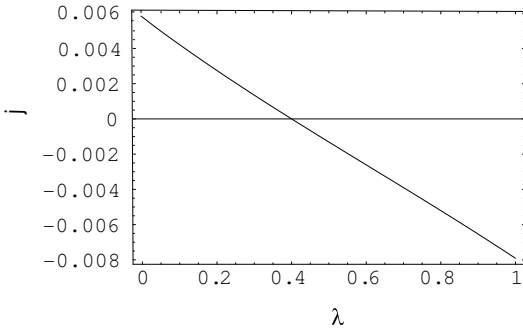$$P_{ref} = \frac{\dot{Q}_c}{\dot{Q}_h - \dot{Q}_c} = \frac{(\varepsilon - 2\lambda)}{3\lambda}.$$ (4.2)

Figure 3: Plot of j versus λ for $\tau = 1$ and $\varepsilon = 2$

From this equation, Eq. (31), we note that in order for the model to function as a refrigerator the upper limit for λ must be $\frac{\varepsilon}{2}$.

The set of points in the parameter space at which current changes its direction differentiates the domain of operation of the model as a refrigerator from that as a heat engine. Using the expression for J, Eq. (24), the value of λ at which the current reversal takes place is given by

$$\lambda = \frac{\varepsilon\tau}{(2\tau + 3)}. \tag{4.3}$$

When we evaluate the values of both η and P_{ref} as we approach this boundary determined by Eq. (32), we find that they are exactly equal to the respective values for the Carnot efficiency and the Carnot COP: $\lim_{J \to 0^+} \eta = \frac{(T_h - T_c)}{T_h}$ and $\lim_{J \to 0^-} P_{ref} = \frac{T_c}{(T_h - T_c)}$. This clearly demonstrates that the boundary at which current is zero corresponds to the quasistatic limit be it from the heat engine side or from the refrigerator side.

In analyzing the operation of our model above, we have identified that when

$$0 < \lambda < \frac{\varepsilon\tau}{(2\tau + 3)}, \tag{4.4}$$

the model works as a heat engine while it works as a refrigerator when

$$\frac{\varepsilon\tau}{(2\tau + 3)} < \lambda < \frac{\varepsilon}{2}. \tag{4.5}$$

Therefore, the model neither works as a heat engine nor as a refrigerator when

$$\lambda > \frac{\varepsilon}{2}. \tag{4.6}$$

Figure 4 shows the three regions in the λ-τ parameter space in which the model operates as a heat engine, a refrigerator and as neither of the two for fixed value of $\varepsilon = 4$. On the other hand, Fig. 5 shows these three regions in the λ-ε parameter space for fixed value of $\tau = 1$.

Let us now further investigate how the current, efficiency and performance of the refrigerator behave as a function of the different parameters characterizing the model. The plot of η versus λ shows that, the efficiency , η, increases with increase in λ until it attains its maximum value (Carnot efficiency) as shown in Fig. 6a. On other hand, the plot of P_{ref} versus λ shows that within
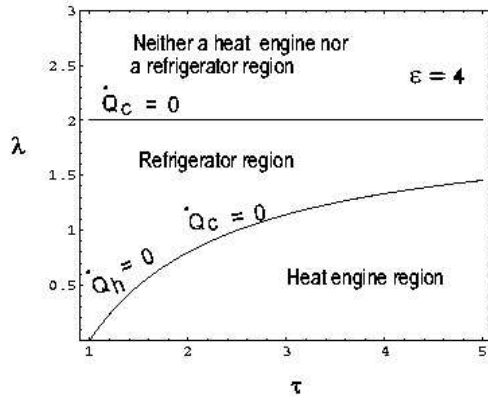
Figure 4: Plot showing the three regions of operation of the model in the λ-τ parameter space for $\varepsilon = 4$
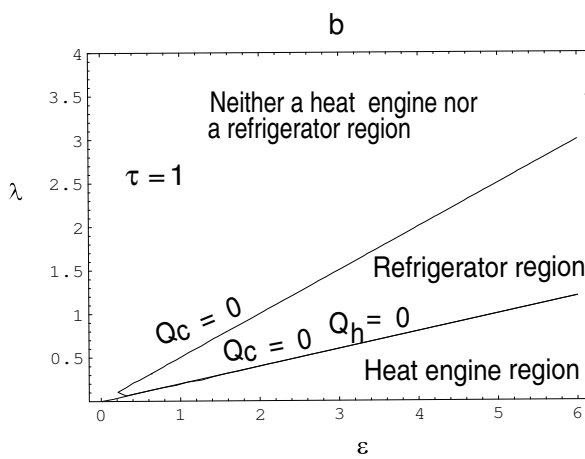

Figure 5: Plot showing the three regions of operation of the model in the λ-ε parameter space for $\tau = 1$
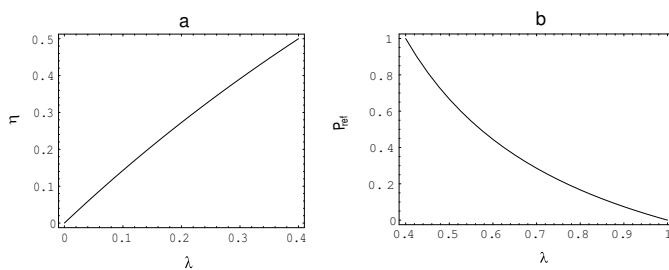
Figure 6: (a) Plot of η versus λ for $\varepsilon = 2$ and $\tau = 1$ (b) Plot of P_{ref} versus λ for $\varepsilon = 2$ and $\tau = 1$
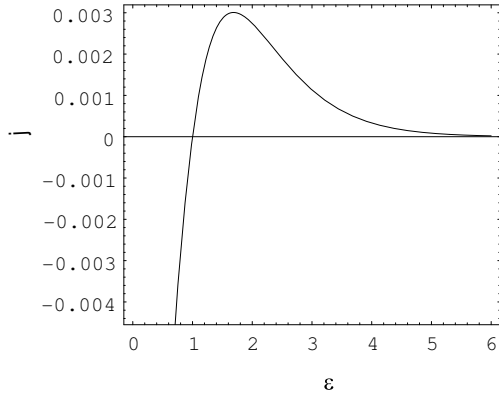
Figure 7: Plot of j versus ε for $\lambda = .2$ and $\tau = 1$

the range where the model works as a refrigerator, coefficient of performance of the refrigerator, P_{ref}, decreases from its maximum value (Carnot refrigerator) as λ increases (see Fig. 6b).

Figure 7 shows how the current j behaves as a function of ε. The figure shows the presence of maximum current at a certain finite value of ε for a fixed τ and λ. This point corresponds to maximum power delivery at which the engine operates with maximum power efficiency, η_{MP}. Let us compare the value η_{MP} of our engine with the corresponding value of an endoreversible engine. For endoreversible engine which exchanges heat linearly at a finite rate with two reservoirs, Curzon and Ahlborn [10, 11] showed that the efficiency at maximum power, η_{CA}, is given by

$$\eta_{CA} = 1 - \sqrt{\left(\frac{T_c}{T_h}\right)}. \tag{4.7}$$

Figure 8 shows how the efficiency of our model heat engine when it operates with maximum power, η_{MP}, and that of η_{CA} behave as a function of τ. The two plots show that as τ increases from zero the value of η_{CA} stays less than that of η_{MP} up to a certain value of τ where they both attain the same value. Beyond that value of τ, the value of η_{CA} becomes larger than that of η_{MP} and their difference monotonically increases with τ. When we compare the two efficiencies, η_{MP} and η_{CA}, η_{CA} is found by assuming linear heat conductivity while η_{MP} is obtained without taking any assumption. This illustrates that η_{MP} is valid for the entire range in the allowed parameter space while η_{CA} is specific and has limited significance.

Let us next compare Carnot efficiency, η_{CAR}, with what is called optimized efficiency, η_{OPT}. One extreme is for an engine to perform a task extremely slowly by utilizing minimum possible energy. The other extreme is to perform the same task at the shortest possible time but at the expense of utilizing large amount of energy. Finding the operating condition where there is the best compromise between these two extremes and evaluating its corresponding efficiency is what we mean by optimized efficiency, η_{OPT}.

The η_{OPT} for our model can be found using the argument stated by Herǹandez. *et al* [12]. We briefly summarized the method of Herǹandez. *et al* [12] in our earlier work [4]. The optimized efficiency, η_{OPT}, lies between maximum efficiency and efficiency under maximum power and it is
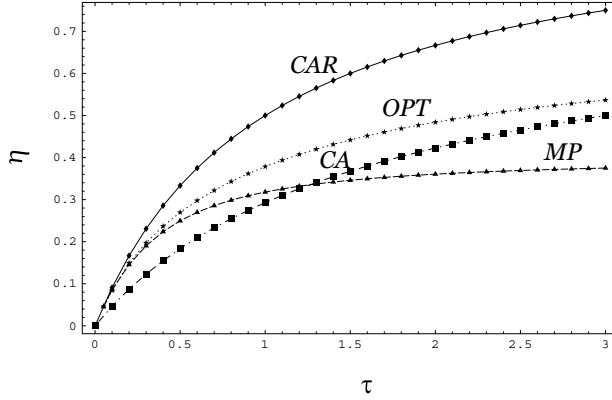
Figure 8: Plots of η_{CA}, η_{MP}, η_{OPT} and η_{CAR} versus τ, where the model engine is put to function at $\lambda = 0.2$ while ε is fixed depending on whether it is working at either maximum power or optimized efficiency
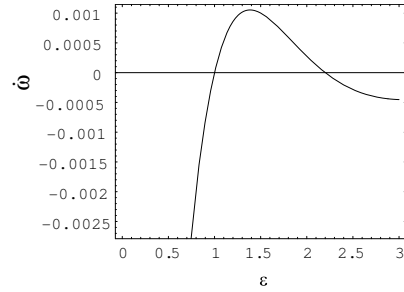

Figure 9: Plot of $\dot{\omega}$ versus ε for $\lambda = .2$ and $\tau = 1$

given by optimizing

$$\dot{\Omega} = 2\dot{W} - \frac{(T_h - T_c)}{T_h}\dot{Q}_h. \tag{4.8}$$

The plot of the dimensionless quantity $\dot{\omega} = \frac{\dot{\Omega}}{\Gamma T_C}$ versus ε in Fig. 9 shows that the function definitely has optimum value at finite ε. Evaluating the efficiency at this particular point in the parameter space gives us the optimized efficiency, η_{OPT}. We plot η_{OPT} and η_{CAR} in the same Figure 8 that we plot the other efficiencies. The plots of η_{OPT} and η_{CAR} versus τ show that η_{OPT} lies between η_{MP} and η_{CAR}. This undeniably illustrates that the operation of the engine at optimized efficiency is a compromise between fastest transport and minimum energy cost.

5. Summary and Conclusion

In this work, we introduced an exactly solvable model of a heat engine with minimum ingredients. We obtained closed form expressions for current, efficiency and COP of the model. We showed that at quasistatic limit the values of both efficiency and COP go to that of Carnot efficiency and Carnot COP, respectively. We then explored the basic properties of the microscopic heat engine by varying the parameters describing the model. We further studied the efficiency when the engine operates with maximum power and compared this efficiency with those values one gets by using the finite-rate linear heat exchange assumption of Curzon and Ahlborn [10, 11]. The results of

11

optimized efficiencies of the model are also reported. It is worth to note that the particle walks in non-viscous medium. Hence the model does not work as a heat engine in the absence of external load. In the presence of external load, even though the model and its corresponding dynamics is completely different from the one we studied earlier, there is a qualitative agreement between this work and the earlier work. Therefore, one can take this work as independent check of the results we found in the previous work on Brownian heat engine [4].

Acknowledgments

References

[1] B. Andresen, P. Salamon, and R.S. Berry, Physics Today, September 1984.

[2] R.D. Astumian, P. Hanggi, Phys. Today **55**, 33 (2002).

[3] P. Reimann, Phys. Rep. **361**, 57, (2002).

[4] Mesfin Asfaw and Mulugeta Bekele, Eur. Phys. J. B **38** , 457, (2004).

[5] C. Jarzynski and O. Mazonka, Phys. Rev. E **59**, 6448 (1999).

[6] R. P. Feynman, R. B. Leighton and M. Sands, *The Feynman Lectures on Physics* (Addison-Wesley, Reading, MA, 1963), Vol. 1.

[7] N. Metropolis *et al*. J. Chem. Phys. **21**, 1087 (1953) N0=" 9, 62'.'

[8] I. Derenyi and R. D. Astumian, Phys. Rev. E **59**, R6219 (1999).

[9] I. Derenyi, M. Bier and R. D. Astumian, Phys. Rev. Lett. **83**, 903 (1999).

[10] F.L. Curzon, B. Ahlborn, Am. J. Phys. **43**, 22 (1975).

[11] P. Salamon *et al*., Energy (Oxford) **26**,307 (2001).

[12] Calvo Hernández A. *et al*., Phys. Rev. E, **63**, 037102 (2001).